

# The Role of AI in Image De-Identification

AI's ability to detect demographics

Judy Gichoya, MD MS

Director, HITI Lab

Assistant Professor, Department of Radiology

Emory University



EMORY  
UNIVERSITY

# Disclosures

- ACR
  - AI advisory council
- RSNA
  - Associate Editor - Radiology AI Trainee Editorial Board
  - CIRE Committee member
- SIIM
  - Co-chair – Research Committee
  - Board member
- NSF grant
  - FW-HTF-RM: Measuring learning gains in man-machine assemblage when augmenting radiology work with artificial intelligence
- HL7 and AHLI Board member
  - Association for Health Learning and Inference
- Softbrew LTD
  - Consulting on Global Health /Clinical informatics
- Funding –
  - NBIB MIDRC / COVID -19 Data repository
  - Clairity Consortium
  - NIH AIM AHEAD pilot grant
  - RSNA Health disparities grant
  - DeepLook

# RECAP



The Lancet Digital Health

Available online 11 May 2022

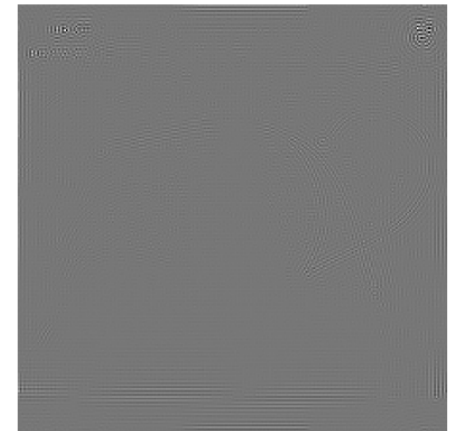
In Press, Corrected Proof



Articles

## AI recognition of patient race in medical imaging: a modelling study

Judy Wawira Gichoya MD<sup>a,\*,</sup> Imon Banerjee PhD<sup>c</sup>, Ananth Reddy Bhimoreddy MS<sup>a</sup>, John L Burns MS<sup>d</sup>, Leo Anthony Celi MD<sup>e,\*,</sup> Li-Ching Chen BS<sup>h</sup>, Ramon Correa BS<sup>c</sup>, Natalie Dullerud MS<sup>i</sup>, Marzyeh Ghassemi PhD<sup>e,\*,</sup> Shih-Cheng Huang<sup>j</sup>, Po-Chih Kuo PhD<sup>h</sup>, Matthew P Lungren MD<sup>j</sup>, Lyle J Palmer PhD<sup>k,\*,</sup> Brandon J Price MD<sup>m</sup>, Saptarshi Purkayastha PhD<sup>d</sup>, Ayis T Pyrros MD<sup>n</sup>, Lauren Oakden-Rayner MD<sup>k</sup>, Chima Okechukwu MS<sup>o</sup> ... Haoran Zhang MS<sup>i</sup>



- 1) Performance of deep learning models to detect race from medical images across modalities and external datasets
- 2) Assessment of possible anatomic and phenotype confounders such as body habitus and disease distribution
- 3) Investigation into underlying mechanisms by which AI models can recognize race.



## Race detection in radiology imaging

### Chest x-ray (internal validation)\*

|  |                  |
|--|------------------|
| MXR (Resnet34, Densenet121)                  | 0.97, 0.94       |
| CXP (Resnet 34)                              | 0.98             |
| EMX (Resnet34, Densenet121, EfficientNet-B0) | 0.98, 0.97, 0.99 |

### Chest x-ray (external validation)\*

|                        |            |
|------------------------|------------|
| MXR to CXP, MXR to EMX | 0.97, 0.97 |
| CXP to EMX, CXP to MXR | 0.97, 0.96 |
| EMX to MXR, EMX to CXP | 0.98, 0.98 |

### Chest x-ray (comparison of models)†

|               |                                  |
|---------------|----------------------------------|
| MXR, CXP, EMX | Multiple results (appendix p 26) |
|---------------|----------------------------------|

### CT chest (internal validation)\*

|                     |            |
|---------------------|------------|
| NLST (slice, study) | 0.92, 0.96 |
|---------------------|------------|

### CT chest (external validation)\*

|                               |            |
|-------------------------------|------------|
| NLST to EM-CT (slice, study)  | 0.80, 0.87 |
| NLST to RSPECT (slice, study) | 0.83, 0.90 |

### Limb x-ray (internal validation)\*

|     |      |
|-----|------|
| DHA | 0.91 |
|-----|------|

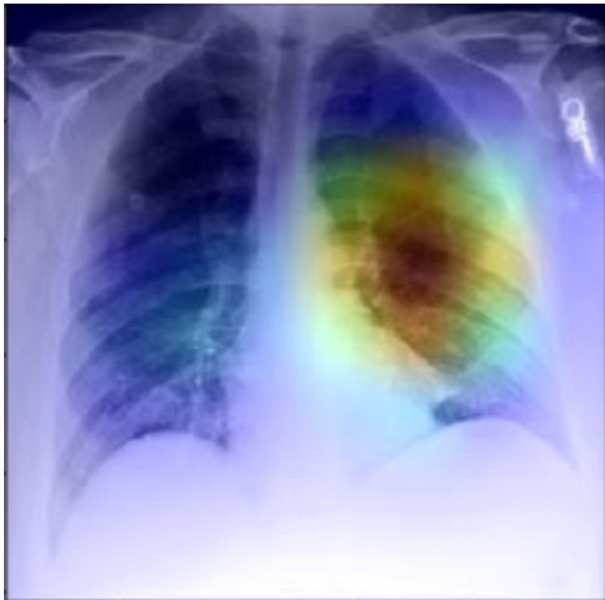
### Mammography\*

|                         |            |
|-------------------------|------------|
| EM-Mammo (image, study) | 0.78, 0.81 |
|-------------------------|------------|

### Cervical spine x-ray\*

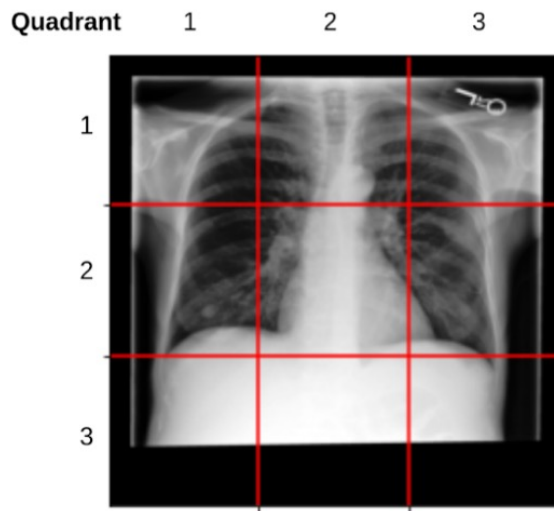
|       |      |
|-------|------|
| EM-CS | 0.92 |
|-------|------|

# Image Obscuration

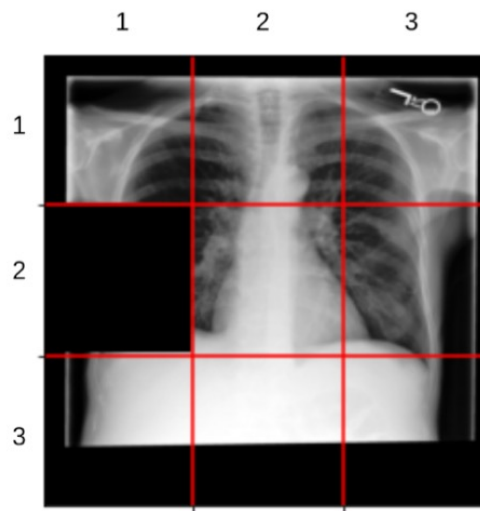


|                          | Asian | Black | White |
|--------------------------|-------|-------|-------|
| MXR Densenet121-Original | 0.93  | 0.94  | 0.94  |
| MXR Densenet121-Masked   | 0.88  | 0.79  | 0.79  |

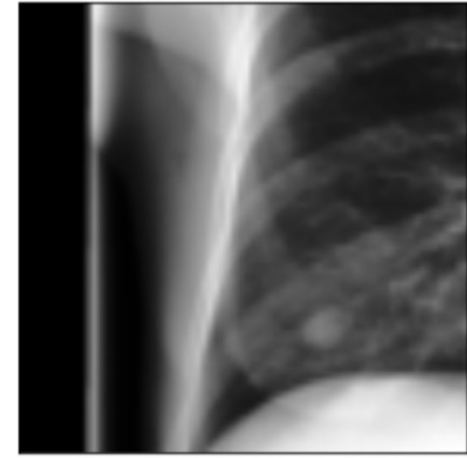
# Patch predictions and exclusions



a) Original image

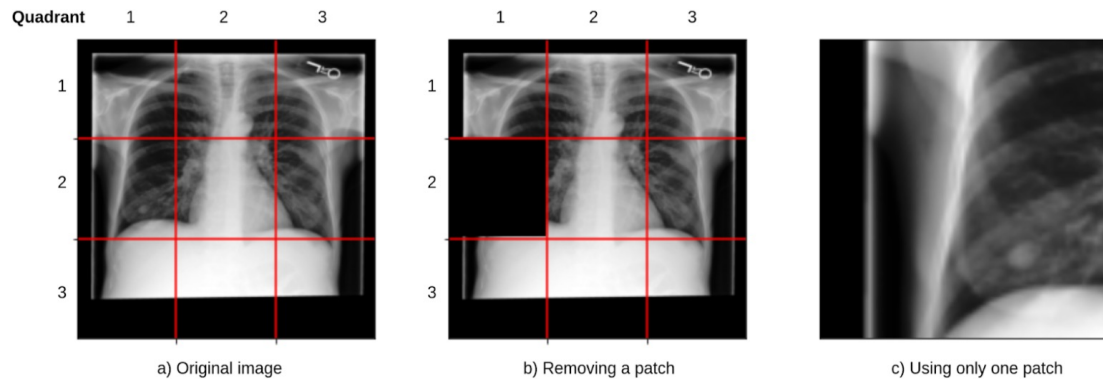


b) Removing a patch



c) Using only one patch

# Patch predictions and exclusions



Patch exclusion

| Quadrant | 1    | 2    | 3    |
|----------|------|------|------|
| 1        | 0.87 | 0.88 | 0.87 |
| 2        | 0.81 | 0.82 | 0.81 |
| 3        | 0.75 | 0.60 | 0.75 |

Single Patch Training

| Quadrant | 1    | 2    | 3    |
|----------|------|------|------|
| 1        | 0.91 | 0.90 | 0.91 |
| 2        | 0.91 | 0.91 | 0.91 |
| 3        | 0.91 | 0.91 | 0.91 |

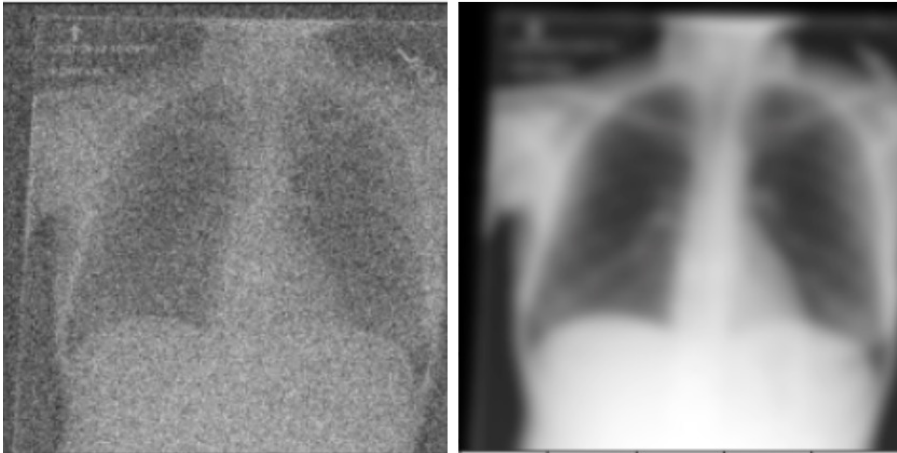
# Anatomic Segmentation



|                          | Asian | Black | White |
|--------------------------|-------|-------|-------|
| MXR Densenet121-Original | 0.93  | 0.94  | 0.94  |
| MXR Densenet121-Non lung | 0.87  | 0.85  | 0.87  |
| MXR Densenet121-Lung     | 0.68  | 0.74  | 0.73  |



# Image Degradation Experiments



|                          | Asian | Black | White |
|--------------------------|-------|-------|-------|
| MXR Densenet121-Original | 0.93  | 0.94  | 0.94  |

|                         |      |      |      |
|-------------------------|------|------|------|
| MXR Densenet121-Noisy   | 0.64 | 0.72 | 0.70 |
| MXR Densenet121-Blurred | 0.59 | 0.64 | 0.62 |

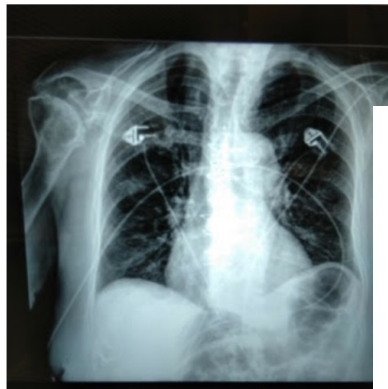
# Image Degradation Experiments

Model trained on CheXphoto performance compared to CheXpert

Original (CheXpert)

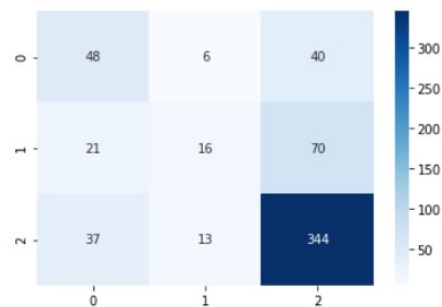


CheXphoto



CheXphoto

|       | AUC  |
|-------|------|
| Asian | 0.81 |
| Black | 0.77 |
| White | 0.80 |



CheXpert

|       | AUC  |
|-------|------|
| Asian | 0.90 |
| Black | 0.94 |
| White | 0.89 |

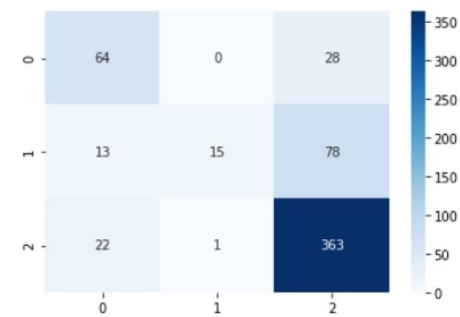
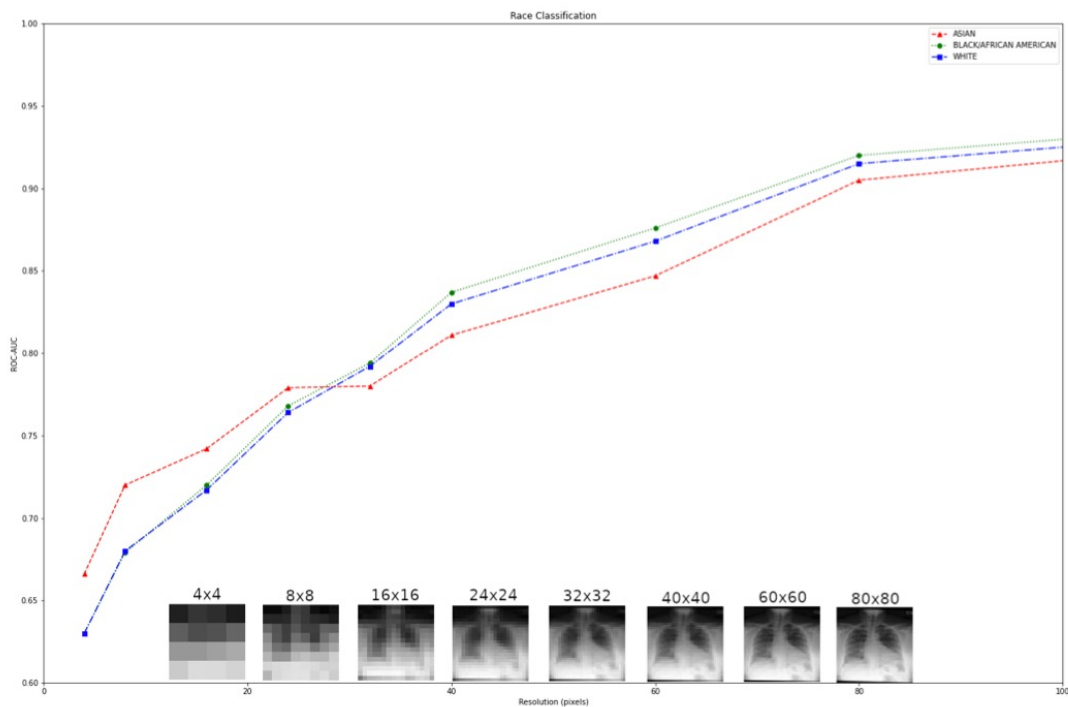
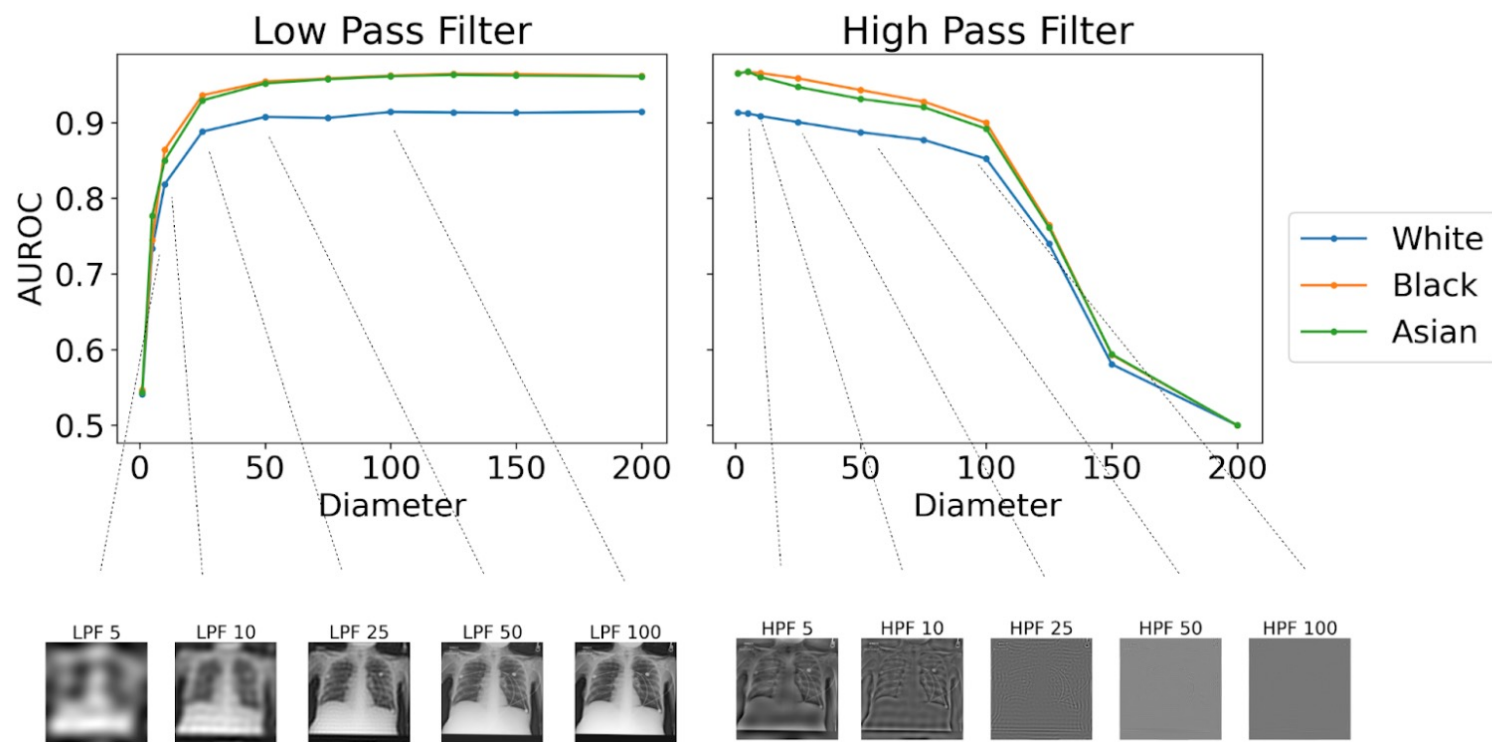


# Image Degradation Experiments

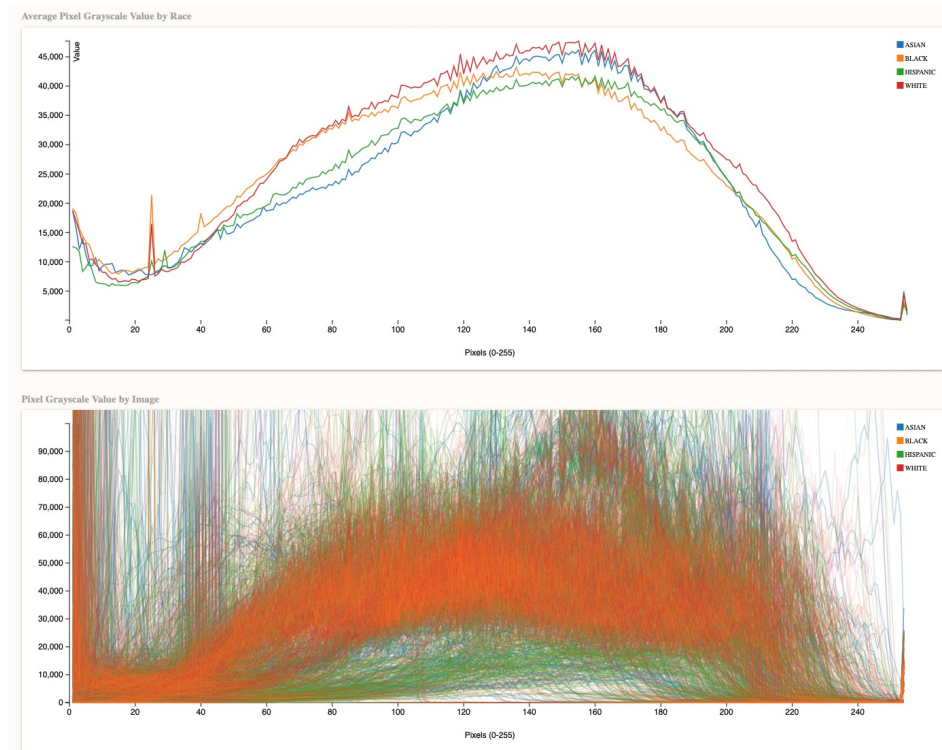


| Race  | Resolution |      |      |      |      |      |      |      |      |      |      |      |
|-------|------------|------|------|------|------|------|------|------|------|------|------|------|
|       | 4          | 8    | 16   | 24   | 32   | 40   | 60   | 80   | 160  | 240  | 320  | 512  |
| Asian | 0.66       | 0.72 | 0.74 | 0.78 | 0.78 | 0.81 | 0.85 | 0.90 | 0.95 | 0.96 | 0.97 | 0.98 |
| Black | 0.63       | 0.68 | 0.72 | 0.77 | 0.79 | 0.84 | 0.88 | 0.92 | 0.96 | 0.97 | 0.97 | 0.98 |
| White | 0.63       | 0.68 | 0.72 | 0.76 | 0.79 | 0.83 | 0.87 | 0.92 | 0.96 | 0.96 | 0.97 | 0.97 |

# Image Degradation Experiments



# Data Visualization: Pixel Color Averages by Race in Chest X-Ray



<https://ai-vengers.web.app>



**INDIANA UNIVERSITY**  
SCHOOL OF MEDICINE

# Pixel Intensity Averages by Race in Chest X-Ray

John Burns<sup>1</sup>, Zachary Zaiman<sup>2</sup>, Gaoxiang Luo<sup>3</sup>, Le Peng<sup>3</sup>, Brandon Price<sup>4</sup>, Garric Mathias<sup>1</sup>, Vijay Mittal<sup>1</sup>, Akshay Sanage<sup>1</sup>, Jack Vanschaik<sup>1</sup>, Christopher Tignanello<sup>3</sup>, Sunandan Chakraborty<sup>1</sup>, Judy Wawira Gichoya<sup>2</sup>, Saptarshi Purkayastha<sup>1</sup>

<sup>1</sup> Indiana University Purdue University at Indianapolis, Indianapolis IN 46202, USA; <sup>2</sup> Emory University, Atlanta GA 30322, USA;

<sup>3</sup> University of Minnesota Twin Cities, Minneapolis MN 55455, USA; <sup>4</sup> University of Florida College of Medicine, Gainesville FL 32610, USA

## ABSTRACT

Recent work using neural networks has shown that self-reported race is embedded in medical imaging. We seek an understanding of the mechanism that reveals race within medical imaging, investigating the possibility that race is embedded within the individual pixel intensities of grayscale medical images.

Using datasets from 3 institutions and MIMIC-CXR with a combined total of 298,827 images, we remove all image structure, count how many times each intensity value appears, and standardize to percent per image (PPI). Visual analysis, statistical tests, and machine learning processes show that intensity PPI contains self-reported race information. The best performing model using gradient boosted trees can predict with an AUROC of 77.24. We investigate confounders of body habitus using Body Mass Index (BMI) and scanner specific settings by limiting to one scanner. Neither factor significantly influences the model.

## BACKGROUND

Medical imaging artificial intelligence (AI) models produce racial disparities [2, 3]. There is potential for discriminatory harm if we assume that AI models are agnostic to race. Understanding the relationship between race and medical imaging AI models is important [4]. AI recognition of patient race in medical imaging: a modelling study authors found that self-reported race is trivially predictable by AI models. They show that AI models can predict self-reported race across multiple imaging modalities, various datasets, and diverse clinical tasks.

These results are surprising, particularly as this task has not been shown possible for human experts. This capability is trivially learned and therefore likely to be present in many medical image analysis models, providing a direct vector for the reproduction or exacerbation of the racial disparities that already exist in medical practice [1].

## MATERIALS and METHODS

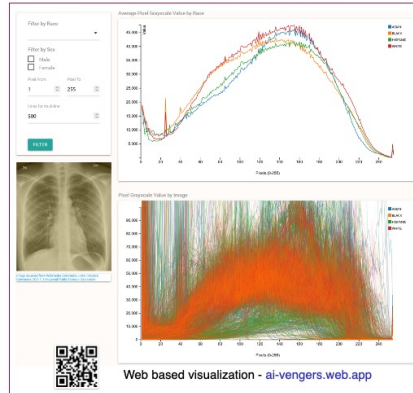
The dataset consists of 3 large academic health centers and one publicly available dataset MIMIC-CXR [5] and is 298,827 images total.

- Institution 1 has 2 datasets: 1 year at hospital W (1.1); and 1 year at hospitals X, Y, Z (1.2) – each limited to the top 10% diverse X-Ray devices.
- Institution 2 has 5 datasets: 1 uncontrolled (2.1); and 4 limited to a single X-Ray device categorized by body habitus using BMI – underweight (2.2), normal (2.3), overweight (2.4), and obese (2.5).
- Institution 3 has 1 uncontrolled dataset (3).

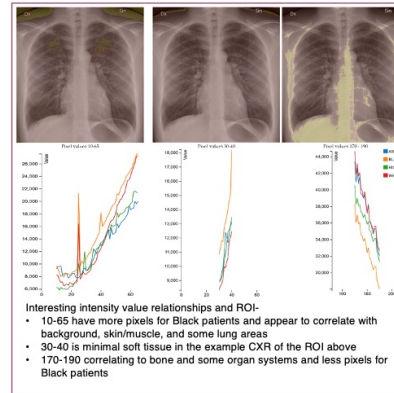
Data is converted from DICOM to 8-bit PNG format, then each intensity value is counted, and then the counts are converted to PPI to normalize for size of image.

Visualizations, MANOVA, and machine learning are applied for individual datasets and all combined

## VISUALIZATION RESULTS



## REGIONS OF INTEREST



Interesting intensity value relationships and ROI:

- 10-65 have more pixels for Black patients and appear to correlate with background, skin/muscle, and some lung areas
- 30-40 is minimal soft tissue in the example CXR of the ROI above
- 170-190 correlating to bone and some organ systems and less pixels for Black patients

## SUMMARY

- ANOVA/MANOVA results show that there is a significant relationship between intensity PPI and self-reported race
- Visualization of this data proved critical for analysis and idea generation
- FFN were unable to accurately predict self-reported race from PPI
- Gradient Boosted Trees achieved a best AUROC of 77.24%, showing that PPI can be used to predict race
- There is little evidence that modality configurations or BMI are correlated to model performance
- Identifying race using pixel gray-scale values without image structure is novel
- Race-bias information exists in x-ray images, even when image structure is removed

## CONCLUSIONS

Prior studies utilized CNN and the full image to achieve high AUROC in race prediction. We have shown predictive value in gray-scale PPI for self-reported race classification. Future work includes:

- Histogram normalization to remove race from images and evaluating for clinically-relevant information loss
- Review of additional modalities and body parts for similar information
- Using 3D CT, segment body parts and evaluate PPI for regions of images

Diversity of data in medical imaging AI is important. It is unknown how racial bias affects medical imaging AI – though it is shown to affect multiple other medical disciplines. Researchers and vendors should publish training/testing dataset information inclusive of diversity-performance information.

## REFERENCE

- Gichoya, Judy Wawira et al. "AI recognition of patient race in medical imaging: a modelling study." *The Lancet. Digital health*, vol. 4, no. 6, (2022): e406-e414. doi:10.1016/S2589-7500(22)00063-2.
- Pearson, D. M., Culler, J., Leskovec, S., Mullamathan, and Z. Obermeyer. "An algorithmic approach to reducing unexplained pain disparities in underserved populations." (in eng). *Nat Med*, vol. 27, no. 1, pp. 136-140, Jan 2021. doi:10.1038/s41591-020-11192-7.
- Seyyed-Kalantari, G., Liu, M., McDermott, I. Y., Chen, and M. Ghaseini. "Chickadee: Fairness gaps in deep chest X-ray classifiers." (in eng). *Pac Symp Biocomput*, vol. 26, pp. 232-243, 2021.
- A. Tariq et al. "Current Clinical Applications of Artificial Intelligence in Radiology and Their Best Supporting Evidence." (in eng). *J Am Coll Radiol*, vol. 17, no. 11, pp. 1371-1381, Nov 2020. doi:10.1016/j.jacr.2020.08.018.
- T. J. P. Alstair et al. "MIMIC-CXR-JPG, a large publicly available database of labeled chest radiographs." *arXiv.org*, 2019. [Online]. Available: <https://arxiv.org/abs/1901.07042>.

## STATISTICAL RESULTS

| Dataset             | ANOVA      |         | MANOVA  |         | MANOVA Balanced |         |        |
|---------------------|------------|---------|---------|---------|-----------------|---------|--------|
|                     | # F < 0.05 | # F > 2 | F-Value | P-Value | F-Value         | P-Value |        |
| 1.1                 | 217        | 234     | 762     | 1.49    | 0.0000          | 1.14    | 0.0119 |
| 1.2                 | 184        | 210     | 762     | 1.22    | 0.0000          | 1.16    | 0.0031 |
| 1 - All             | 215        | 223     | 762     | 1.64    | 0.0000          | 1.30    | 0.0000 |
| 2.1                 | 245        | 252     | 508     | 3.23    | 0.0000          | 2.99    | 0.0000 |
| 2.2                 | 138        | 158     | 762     | 1.38    | 0.0000          | 0.93    | 0.7726 |
| 2.3                 | 241        | 244     | 762     | 2.65    | 0.0000          | 1.13    | 0.0140 |
| 2.4                 | 241        | 246     | 762     | 2.88    | 0.0000          | 1.36    | 0.0000 |
| 2.5                 | 226        | 239     | 762     | 2.73    | 0.0000          | 1.18    | 0.0015 |
| 2 - All             | 245        | 250     | 762     | 3.38    | 0.0000          | 2.82    | 0.0000 |
| 3                   | 220        | 237     | 508     | 2.58    | 0.0000          | 1.67    | 0.0000 |
| MIMIC               | 243        | 246     | 762     | 7.04    | 0.0000          | 2.90    | 0.0000 |
| Combined - No MIMIC | 248        | 249     | 762     | 8.63    | 0.0000          | 3.37    | 0.0000 |
| Combined - All      | 255        | 255     | 762     | 35.64   | 0.0000          | 11.07   | 0.0000 |

- ANOVA –
- With 95% confidence we can reject the null hypothesis for most grayscale values.
  - As a combined dataset 255 of 256 values are  $p < 0.05$  and 255 of 256 values  $F > 2$ .
  - ANOVA assumes variables are uncorrelated, many pixel counts appear to be highly correlated with other pixel counts.
- MANOVA with Bonferroni multiple-comparison adjustment at an  $\alpha=0.05$  –
- All MANOVA tests have significant  $p$  values, indicating that for all source datasets, the pixel percentage distribution is significantly different across different races.
- MANOVA balanced –
- Datasets 1.1, 2.2, 2.3 cannot reject the null hypothesis when classes are balanced.

## MACHINE LEARNING RESULTS

| Dataset             | Binary Black or White |       |                           |          | Binary Black or all  |       |                           |       |      |
|---------------------|-----------------------|-------|---------------------------|----------|----------------------|-------|---------------------------|-------|------|
|                     | Feed Forward Network  |       | Decision Tree (RFGBT/Cat) |          | Feed Forward Network |       | Decision Tree (RFGBT/Cat) |       |      |
|                     | Accuracy              | AUROC | Model                     | Accuracy | AUROC                | Model | Accuracy                  | AUROC |      |
| 1.1                 | 66.9                  | 65.2  | RF                        | 57.3     | 60.6                 | 62.9  | RF                        | 65.3  | 58.3 |
| 1.2                 | 58.8                  | 58.8  | GBT                       | 57.1     | 61.5                 | 63.6  | RF                        | 65.9  | 62.4 |
| 1 - All             | 57.1                  | 58.2  | RF                        | 60.5     | 66.8                 | 64.5  | RF                        | 66.3  | 63.2 |
| 2.1                 | 66.8                  | 65.1  | RF                        | 63.4     | 67.7                 | 67.5  | RF                        | 66.3  | 66.6 |
| 2.2                 | 66.6                  | 64.6  | RF                        | 64.0     | 67.5                 | 54.5  | RF                        | 62.4  | 65.1 |
| 2.3                 | 65.2                  | 65.0  | RF                        | 63.5     | 67.3                 | 62.5  | RF                        | 65.1  | 66.3 |
| 2.4                 | 66.7                  | 62.2  | RF                        | 65.2     | 65.5                 | 65.3  | RF                        | 66.0  | 67.6 |
| 2.5                 | 62.2                  | 65.3  | RF                        | 61.6     | 64.7                 | 60.4  | RF                        | 62.9  | 66.4 |
| 2 - All             | 61.7                  | 64.5  | RF                        | 64.7     | 69.6                 | 62.3  | RF                        | 65.9  | 68.8 |
| 3                   | 67.4                  | 67.9  | RF                        | 78.5     | 74.1                 | 68.5  | RF                        | 71.9  | 72.6 |
| MIMIC               | 60.5                  | 61.2  | GBT                       | 80.4     | 61.7                 | 82.4  | GBT                       | 82.3  | 60.0 |
| Combined - No MIMIC | 58.4                  | 62.5  | GBT                       | 63.0     | 66.8                 | 61.2  | GBT                       | 64.3  | 63.8 |
| Combined - All      | 58.8                  | 65.1  | GBT                       | 75.6     | 70.4                 | 77.8  | GBT                       | 68.5  | 77.3 |

Feed-Forward Networks (FFN) had some success in predicting race, with the highest accuracy of 77.0% and AUROC of 68.4%. In general, model performance follows dataset size. However, Institution 2 single modality/body habitus has better results than the combined.

Gradient Boosted Trees outperformed FFN and other decision trees. The best accuracy of 68.5% and AUROC of 77.2% shows that self-reported race can be identified without image structure.



# Confounders mediate AI prediction of demographics in medical imaging

[Grant Duffy](#), [Shoa L. Clarke](#), [Matthew Christensen](#), [Bryan He](#), [Neal Yuan](#), [Susan Cheng](#) & [David Ouyang](#)



[npj Digital Medicine](#) **5**, Article number: 188 (2022) | [Cite this article](#)

**2207** Accesses | **25** Altmetric | [Metrics](#)

**Table 1.** Demographic characteristics of study participants.

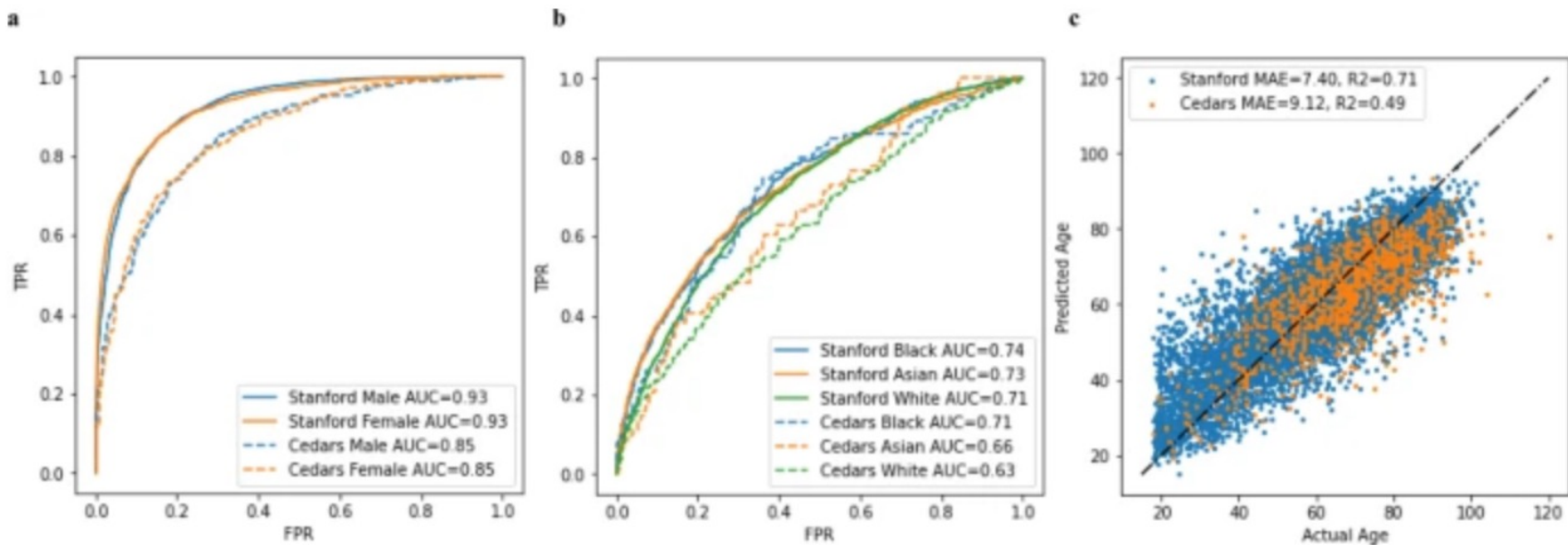
|                              | CSMC             |                  |                       |                | SHC              |
|------------------------------|------------------|------------------|-----------------------|----------------|------------------|
|                              | Apical 4 chamber | Apical 2 chamber | Parasternal long axis | Subcostal      | Apical 4 chamber |
| <i>n</i> , patients          | 28,450           | 25,502           | 28,685                | 23,596         | 99,909           |
| <i>n</i> , videos            | 186,426          | 71,086           | 110,399               | 65,558         | 99,909           |
| Age (mean (SD))              | 66.5 (±16.5)     | 66.7 (±16.5)     | 66.1 (±16.5)          | 66.2 (±16.4)   | 59.9 (±17.7)     |
| Male (%)                     | 15,713 (55.2%)   | 14,093 (55.3%)   | 15,739 (54.9%)        | 12,884 (54.6%) | 55,610 (55.7%)   |
| Race/ethnicity, <i>n</i> (%) |                  |                  |                       |                |                  |
| American Indian              | 65 (0.2%)        | 57 (0.2%)        | 66 (0.2%)             | 56 (0.2%)      | 267 (0.3%)       |
| Asian                        | 2162 (7.6%)      | 1945 (7.6%)      | 2157 (7.5%)           | 1808 (7.7%)    | 14,197 (14.2%)   |
| Black                        | 4058 (14.3%)     | 3681 (14.4%)     | 4156 (14.5%)          | 3322 (14.1%)   | 4826 (4.8%)      |
| Pacific Islander             | 87 (0.3%)        | 82 (0.3%)        | 86 (0.3%)             | 75 (0.3%)      | 1428 (1.4%)      |
| White                        | 19,519 (68.6%)   | 17,444 (68.4%)   | 19,595 (68.3%)        | 16,211 (68.7%) | 56,498 (56.5%)   |
| Other                        | 1980 (7.0%)      | 1790 (7.0%)      | 2021 (7.0%)           | 1659 (7.0%)    | 17,452 (17.5%)   |
| Unknown                      | 579 (2.0%)       | 503 (2.0%)       | 604 (2.1%)            | 465 (2.0%)     | 5241 (5.2%)      |

CSMC Cedars-Sinai Medical Center, SHC Stanford Healthcare.





% White-male 58.5%  
% Black-male 54.1%

**Fig. 1: AI model performance in predicting demographics in with unadjusted training and test datasets.**



ORIGINAL ARTICLE DATA SCIENCE | [VOLUME 19, ISSUE 1, P184-191, JANUARY 01, 2022](#)

# Detecting Racial/Ethnic Health Disparities Using Deep Learning From Frontal Chest Radiography

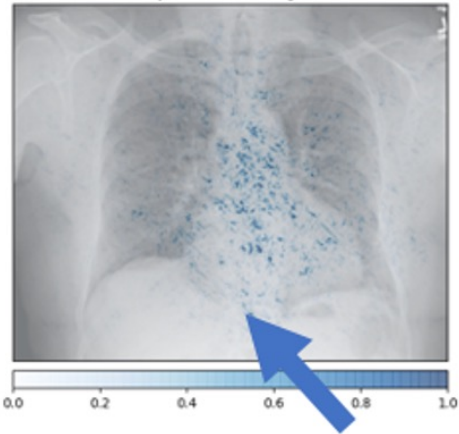
[Ayis Pyrros, MD](#)   • [Jorge Mario Rodríguez-Fernández, MD](#) • [Stephen M. Borstelmann, MD](#) • [Judy Wawira Gichoya, MD](#) • [Jeanne M. Horowitz, MD](#) • [Brian Fornelli, MS](#) • [Nasir Siddiqui, MD](#) • [Yury Velichko, PhD](#) • [Oluwasanmi Koyejo, PhD](#) • [William Galanter, MD, PhD](#) • [Show less](#)

DOI: <https://doi.org/10.1016/j.jacr.2021.09.010> •



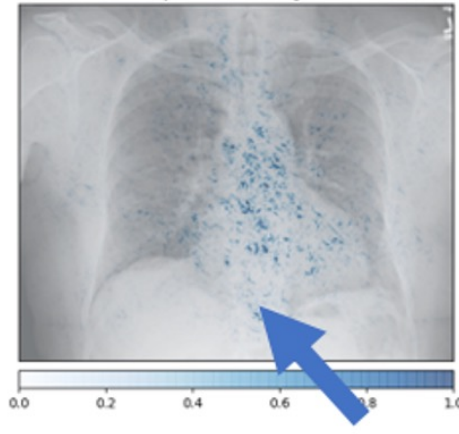
HCC85-CHF

Overlaid Gradient Magnitudes



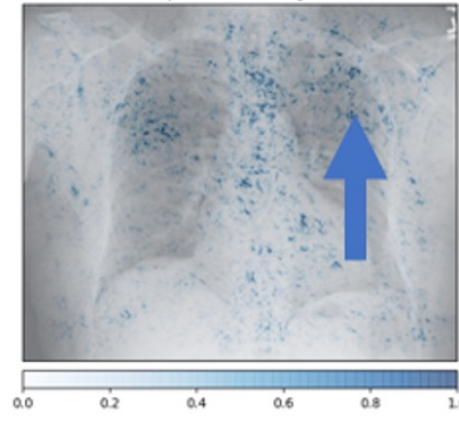
HCC96-Arrhythmia (A.fib)

Overlaid Gradient Magnitudes



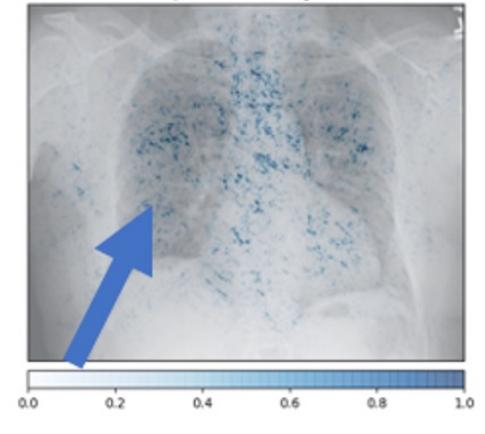
HCC22-Morbid Obesity

Overlaid Gradient Magnitudes



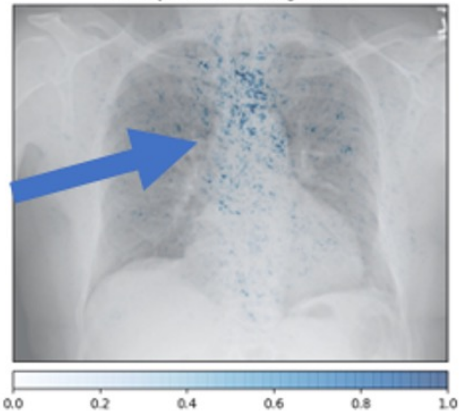
HCC111-COPD

Overlaid Gradient Magnitudes



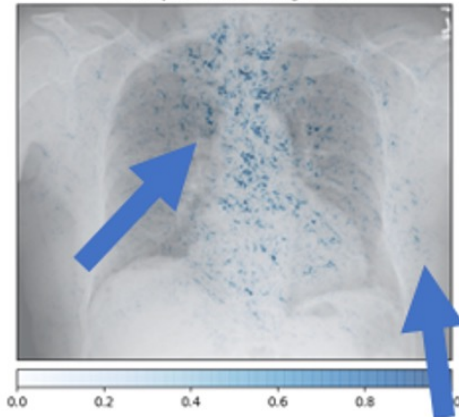
HCC108-Vascular disease

Overlaid Gradient Magnitudes



HCC18-Diabetes

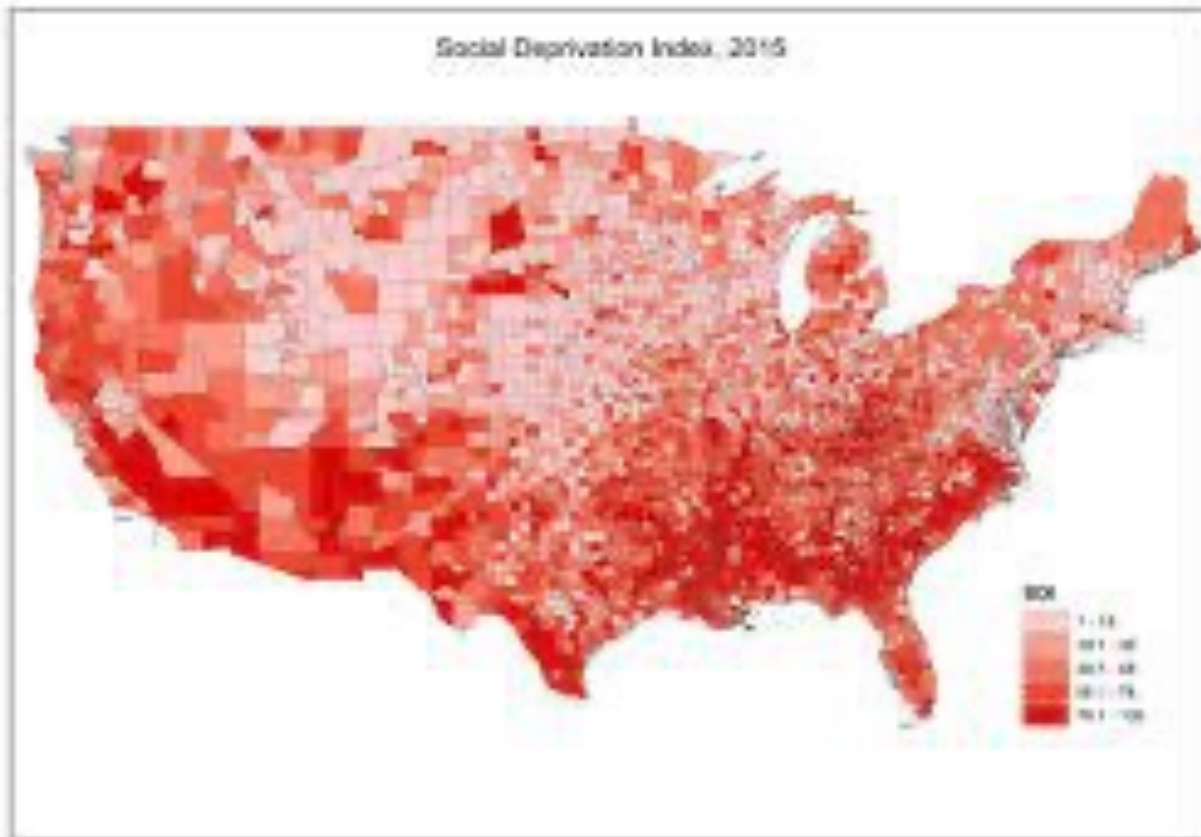
Overlaid Gradient Magnitudes



## One CXR generates six HCC probabilities

- Cardiac arrhythmia maps demonstrate subtle increased activation in the atrial regions
- CHF maps shows enlarged heart
- Vascular disease activation at the aortic knob
- COPD shows increased activation of the lungs
- Diabetes activation in the axillary soft-tissues and aorta

# Social Deprivation Index



NONWHITE:  
ASIAN, BLACK,  
HISPANIC

**AVERAGE AGE 48**

SDI average 45,  
median 40, std 28

Social  
Deprivation  
Index

252 (30%)

114 MALE

138 FEMALE

WHITE

**AVERAGE AGE 52**

SDI average 27,  
median 21, std 23

Social  
Deprivation  
Index

562 (70%)

275 MALE

287 FEMALE

# RECAP



The Lancet Digital Health

Available online 11 May 2022

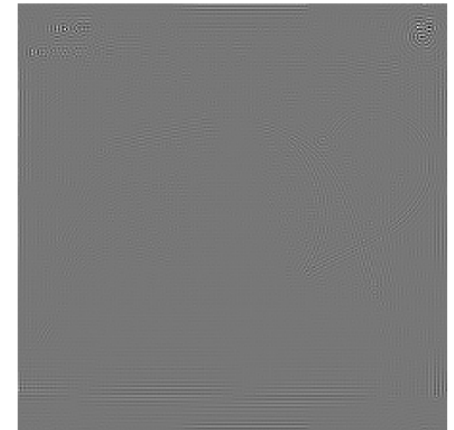
In Press, Corrected Proof



Articles

## AI recognition of patient race in medical imaging: a modelling study

Judy Wawira Gichoya MD<sup>a,\*,</sup> Imon Banerjee PhD<sup>c</sup>, Ananth Reddy Bhimoreddy MS<sup>a</sup>, John L Burns MS<sup>d</sup>, Leo Anthony Celi MD<sup>e,\*,</sup> Li-Ching Chen BS<sup>h</sup>, Ramon Correa BS<sup>c</sup>, Natalie Dullerud MS<sup>i</sup>, Marzyeh Ghassemi PhD<sup>e,\*,</sup> Shih-Cheng Huang<sup>j</sup>, Po-Chih Kuo PhD<sup>h</sup>, Matthew P Lungren MD<sup>j</sup>, Lyle J Palmer PhD<sup>k,\*,</sup> Brandon J Price MD<sup>m</sup>, Saptarshi Purkayastha PhD<sup>d</sup>, Ayis T Pyrros MD<sup>n</sup>, Lauren Oakden-Rayner MD<sup>k</sup>, Chima Okechukwu MS<sup>o</sup> ... Haoran Zhang MS<sup>i</sup>



- 1) Performance of deep learning models to detect race from medical images across modalities and external datasets
- 2) Assessment of possible anatomic and phenotype confounders such as body habitus and disease distribution
- 3) Investigation into underlying mechanisms by which AI models can recognize race.



- [judywawira@emory.edu](mailto:judywawira@emory.edu)
- @judywawira



**Healthcare Innovation and  
Translational Informatics**  
(HITI) Lab at Emory